

# The impact of lens galaxy environments on the image separation distribution

Masamune Oguri,<sup>1,2\*</sup> Charles R. Keeton<sup>3</sup> and Neal Dalal<sup>4†</sup>

<sup>1</sup>*Princeton University Observatory, Peyton Hall, Princeton, NJ 08544, USA.*

<sup>2</sup>*Department of Physics, University of Tokyo, Hongo 7-3-1, Bunkyo-ku, Tokyo 113-0033, Japan.*

<sup>3</sup>*Department of Physics and Astronomy, Rutgers University, 136 Frelinghuysen Road, Piscataway, NJ 08854 USA.*

<sup>4</sup>*Institute for Advanced Study, Einstein Drive, Princeton NJ 08540, USA.*

26 March 2018

## ABSTRACT

We study the impact of lens galaxy environments on the image separation distribution of lensed quasars. We account for both environmental convergence and shear, using a joint distribution derived from galaxy formation models calibrated by galaxy–galaxy lensing data and number counts of massive elliptical galaxies. We find that the external field enhances lensing probabilities, particularly at large image separations; the increase is  $\sim 30\%$  at  $\theta = 3''$  and  $\sim 200\%$  at  $\theta = 5''$ , when we adopt a power-law source luminosity function  $\Phi(L) \propto L^{-2.1}$ . The enhancement is mainly driven by convergence, which boosts both the image separation and magnification bias (for a fixed lens galaxy mass). These effects have been neglected in previous studies of lens statistics. Turning the problem around, we derive the posterior convergence and shear distributions and point out that they are strong functions of image separation; lens systems with larger image separations are more likely to lie in dense environments.

**Key words:** cosmology: theory — dark matter — gravitational lensing

## 1 INTRODUCTION

Strong gravitational lensing offers a unique probe of cosmology and the physical properties of early-type galaxies. For example, the ensemble properties of a well-defined sample of strong lens systems can constrain the cosmological constant (Turner 1990; Fukugita et al. 1990; Kochanek 1996b; Chae 2003; Mitchell et al. 2005), the density profile and evolution of early-type galaxies (Kochanek et al. 2000; Rusin et al. 2003a,b; Rusin & Kochanek 2005), and the amount of substructure in lens galaxies (Metcalf & Madau 2001; Dalal & Kochanek 2002; Kochanek & Dalal 2004). In addition, the image separation distribution of lensed quasars (Turner et al. 1984) probes the efficiency of baryon cooling inside dark matter halos of different masses, and thereby constrains models of galaxy formation (Kochanek & White 2001; Keeton 2001a; Oguri 2002). So far, more than 80 lens systems have been discovered, and the largest homogeneous subsample suitable for statistical studies is the Cosmic Lens All-Sky Survey (CLASS), containing 13 lensed radio sources at image separations  $0'.3 < \theta < 3''$  (Myers et al. 2003; Browne et al. 2003). A larger statistical sample is being constructed from the Sloan Digital Sky Survey (SDSS), which

has already discovered more than 10 new lenses including the largest-separation lensed quasar known to date (Inada et al. 2003; Oguri et al. 2004).

Lensing probability distributions are often computed using a clean spherical lens object without external fields. However, in reality, most observed lenses have non-spherical galaxies, and many require a significant external tidal shear (Keeton et al. 1997). While a portion of the shear may come from fluctuations of matter along the line of sight (Seljak 1994; Bar-Kana 1996; Momcheva et al. 2005), much of it is thought to be associated with mass in the immediate environment of the lens galaxy. Most lens galaxies are early-type, which lie preferentially in dense environments. For instance, Keeton et al. (2000, see also Blandford et al. 2001) used galaxy demographics (specifically, the galaxy luminosity function as a function of type and environment) to predict that at least  $\sim 25\%$  of lens galaxies lie in groups or clusters of galaxies. Indeed, more than 20 lens galaxies are already known to or suspected to be surrounded by groups or clusters (Young et al. 1981; Kundić et al. 1997a,b; Tonry 1998; Fischer et al. 1998; Tonry & Kochanek 1999, 2000; Fassnacht et al. 1999; Hagen & Reimers 2000; Fassnacht et al. 2004; Kneib et al. 2000; Soucail et al. 2001; Faure et al. 2002, 2004; Fassnacht & Lubin 2002; Johnston et al. 2003; Inada et al. 2003; Morgan et al. 2005;

\* E-mail: oguri@astro.princeton.edu

† Hubble Fellow

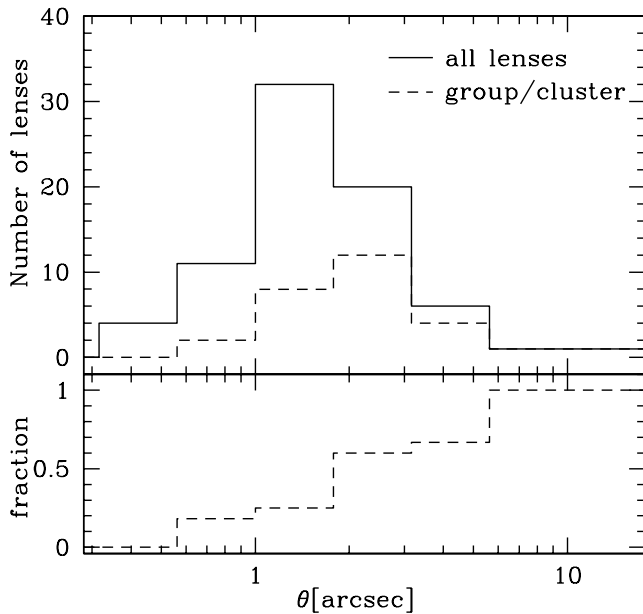


**Figure 1.** Top: Image separation distributions of all lensed quasars (*solid*) and those whose lens galaxies are confirmed to or suspected to lie in a group or cluster (*dashed*). Note that not all lensed quasars have had their environments characterized observationally. Bottom: The fraction of lensed quasars in groups and clusters as a function of image separation.

Oguri et al. 2005; McKean et al. 2005; Momcheva et al. 2005).

Conventional wisdom holds that ellipticity and environment mainly affect the relative numbers of double and quadruple lenses and do not significantly modify the total lensing probability (Kochanek 1996b; Keeton et al. 1997; Rusin & Tegmark 2001; Chae 2003, but see Keeton & Zabludoff 2004). Huterer et al. (2005) showed explicitly that ellipticity and shear change the lensing probability by only a few percent for most source luminosity functions (see also Premadi & Martel 2004). They also found that shear (and to a lesser extent ellipticity) shifts and broadens the distribution of image separations for a given lens galaxy. However, they did not put the two pieces together and discuss changes in the overall image separation distribution. Also, Huterer et al. (and everyone else, for that matter) neglected the effects of external convergence from the environment. External convergence is often omitted from models of individual lenses because the mass sheet degeneracy renders it unmeasurable (Gorenstein et al. 1988; Saha 2000). Nevertheless, theoretical studies show that external convergence affects lensing analyses in many important ways (Keeton & Zabludoff 2004).

There is already some observational evidence that lens galaxy environments affect the image separation distribution. Oguri et al. (2005) found an overabundance of lensed quasars with image separations  $\theta \sim 3''$ . They argued that the excess arises from lens galaxy environments, since many of the  $\theta \sim 3''$  lenses appear to lie in groups or clusters. We extend this consideration to all lensed quasars: Figure 1 shows the image separation distribution for all lensed quasars and for the subset whose lens galaxies lie in groups or clusters. Lens galaxy environment is clearly correlated

with image separation such that lenses with larger separations tend to lie in groups and clusters. The correlation is almost tautological at large separations (say  $\theta > 4''$ ), because it is hard to achieve a large deflection angle without some environmental convergence. But the figure shows a gradual increase of the fraction even at  $\theta < 4''$ . This trend provides further evidence that environmental convergence and shear are important: it contradicts the prediction by Keeton et al. (2000) that, if external convergence and shear are irrelevant, lenses in dense environments should have a *smaller* mean image separation than lenses in the field (because dense environments tend to have a larger ratio of dwarf to giant galaxies than the field).

While these data certainly suggest a connection between environment and lensing, the observational evidence is incomplete because systematic surveys of lens environments have only just begun (see Momcheva et al. 2005). It is therefore valuable to undertake a theoretical analysis of how environments affect lensing probabilities, and what range of environments is expected for lenses with various image separations. In this paper, we compute the lensing effects of shear and convergence associated with matter near the lens galaxy (see also Möller et al. 2002, for the effect of groups on lens statistics). We use a realistic model for the distribution of galaxy environments, which is based on  $N$ -body simulations and the halo occupation distribution and calibrated by observations of galaxy–galaxy lensing and number counts of massive elliptical galaxies (Dalal & Watson 2005). For the lens objects, we assume a singular isothermal sphere (SIS) because it is both simple and a reasonable model for the density profile of lens galaxies (e.g., Cohn et al. 2001; Treu & Koopmans 2002; Koopmans et al. 2003; Rusin & Kochanek 2005). We neglect the ellipticity of lens galaxies for simplicity, but note that the effects of ellipticity are generally smaller than those of external shear (Huterer et al. 2005).

This paper is organized as follows. Section 2 describes the joint probability distribution function of convergence and shear that we use throughout the paper. Section 3 reviews the calculation of lensing probabilities and the image separation distribution. In §4 we examine the image separation distribution from various viewpoints in order to understand how lens environments affect the distribution. Section 5 summarizes our main conclusions. Throughout the paper we assume a concordance cosmology with mass density  $\Omega_M = 0.3$ , cosmological constant  $\Omega_\Lambda = 0.7$ , and dimensionless Hubble parameter  $h = 0.7$ .

## 2 JOINT PDF OF CONVERGENCE AND SHEAR

We consider the probability distribution functions (PDFs) of convergence and shear originating from lens galaxy environments, using the model derived by Dalal & Watson (2005). They placed galaxies in an  $N$ -body simulation using a halo occupation distribution calibrated to match number counts and tangential shear profiles measured for massive elliptical galaxies in the SDSS (see Sheldon et al. 2004), and determined the convergence and shear at each galaxy position. Figure 3 of their paper shows the resulting distributions. The convergence  $\kappa_{\text{ext}}$  and shear  $|\gamma_{\text{ext}}|$  have similar means  $\approx 0.03$ ,

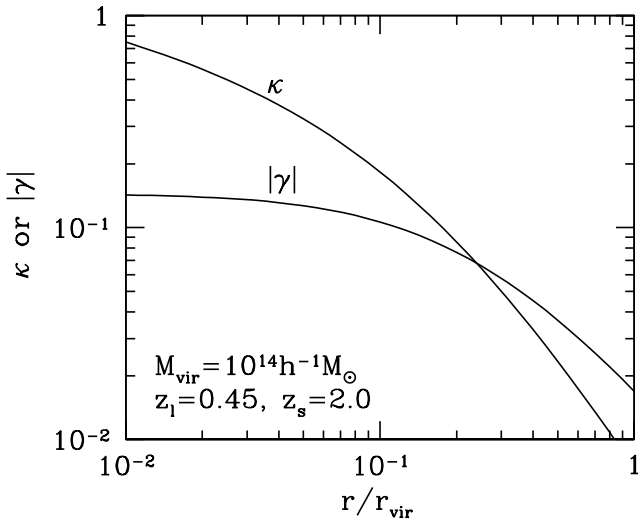


**Figure 2.** Radial profile of convergence and shear in a typical massive dark matter halo. We assume an NFW halo with mass  $M_{\text{vir}} = 10^{14} h^{-1} M_{\odot}$  and concentration parameter  $c = 5.5$ . The lens has redshift  $z_l = 0.45$ , while the source has redshift  $z_s = 2$ .

but very different tails: large convergences ( $\kappa_{\text{ext}} \gtrsim 0.1$ ) are more common than large shears ( $|\gamma_{\text{ext}}| \gtrsim 0.1$ ). There are two reasons for the difference. First, for a typical group or cluster dark matter halo, we expect that a large shear is always accompanied by an even larger convergence. Figure 2 illustrates this idea by showing the convergence and shear profiles for a dark matter halo modeled with an NFW density profile (Navarro et al. 1997); in the central region ( $\kappa, |\gamma| \gtrsim 0.1$ ), we see that  $\kappa > |\gamma|$ .<sup>1</sup> Second, convergence and shear sum differently when there are multiple perturbers. The probability distribution of convergence is highly skewed, with a tail extending to large positive values but no corresponding tail at large negative values. In contrast, the distributions of both shear components are symmetric about zero. Thus, a large convergence provided by one perturber cannot be canceled by contributions from other perturbers, while large shear values can be canceled. As we shall see, the longer tail of convergence is one reason that convergence is more important than shear.

Figure 2 also implies that convergence and shear are not independent but rather correlated. Therefore in this paper we consider the *joint* PDF of convergence and shear, which is shown in Figure 3. The correlation between  $\kappa_{\text{ext}}$  and  $|\gamma_{\text{ext}}|$  is quite evident, particularly for large values.

Although the environment distribution was derived for a lens redshift  $z_l = 0.45$ , we assume little evolution in the elliptical galaxy population over the range  $0 \lesssim z \lesssim 1$  (see Schade et al. 1999; Im et al. 2002; Ofek et al. 2003; Chae & Mao 2003). Thus, we simply extrapolate the surface mass density associated with environment to all redshifts. Since convergence and shear depend on the surface

<sup>1</sup> More generally, for a power-law density profile  $\rho(r) \propto r^{-\eta}$ , the convergence and shear are related as  $|\gamma|/\kappa = |\eta - 1|/|3 - \eta|$ . Therefore the argument holds for different mass profiles, as long as they have inner profiles that are shallower than the isothermal sphere ( $\eta = 2$ ).

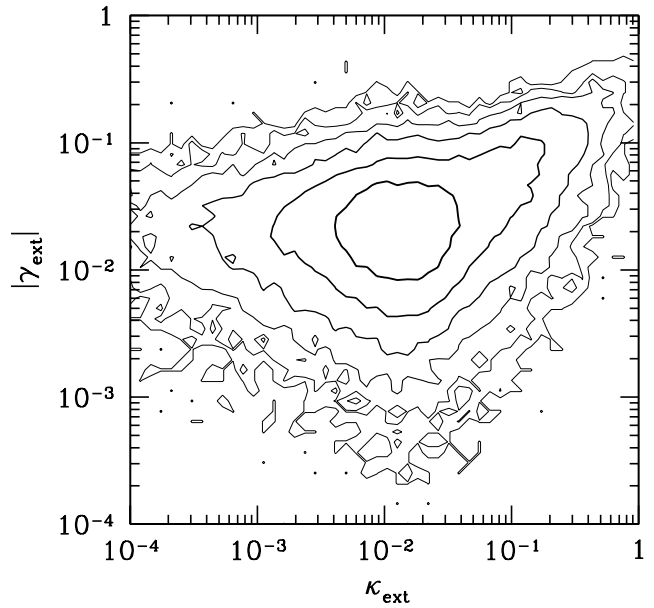


**Figure 3.** Contours of the joint PDF  $p(\kappa_{\text{ext}}, |\gamma_{\text{ext}}|)$  of external convergence and shear derived by Dalal & Watson (2005), assuming redshifts  $z_l = 0.45$  and  $z_s = 2$ . Contours are spaced by 0.5 dex, with thicker lines indicating higher probabilities.

mass density in units of the critical density for lensing,  $\Sigma_{\text{crit}} \propto D_{os}/(D_{ol}D_{ls})$ , the redshift dependence of the PDF for convergence and shear is straightforward. The PDF was derived for galaxies with a velocity dispersion  $\sigma \sim 216 \text{ km s}^{-1}$ , which is typical for lenses with image separation  $\theta \sim 1''$ , but we apply it to all galaxies. In other words, we neglect any correlation between a galaxy's velocity dispersion and environment. However, we know that galaxies with higher velocity dispersion will tend to reside in denser environments; accordingly, our estimate of environmental effects on wide-splitting lenses is strictly a lower limit. We exclude extreme cases with  $\kappa_{\text{ext}} + |\gamma_{\text{ext}}| \geq 1$ , because those would be categorized as lensing by groups/clusters rather than by a galaxy perturbed by its environment.

### 3 LENS STATISTICS WITH EXTERNAL CONVERGENCE AND SHEAR

We model each lens object as an SIS galaxy with external convergence and shear. The Einstein radius of an SIS with velocity dispersion  $\sigma$  is

$$\theta_E(\sigma) = 4\pi \left( \frac{\sigma}{c} \right)^2 \frac{D_{ls}}{D_{os}}, \quad (1)$$

where  $D_{os}$  and  $D_{ls}$  are, respectively, angular diameter distances from the observer and lens to the source.

The important properties of the lens are the image separation as a function of source position, the lensing cross section, and the magnification bias. We define the image separation  $\theta$  to be the maximum distance between multiple images, which is a well-defined and observable quantity. It is useful to define the normalized separation  $\hat{\theta}$  such that

$$\theta(\mathbf{u}) = \theta_E \hat{\theta}(\mathbf{u}). \quad (2)$$

Note that  $\hat{\theta}(\mathbf{u}) = 2$  for all  $\mathbf{u}$  in the absence of convergence and shear.

We combine the cross section and magnification bias to compute the “biased cross section”,

$$BA = \int \frac{\Phi(L/\mu)}{\Phi(L)} d\mathbf{u} = \int \mu^{\beta-1} d\mathbf{u}, \quad (3)$$

where the integral is over the multiply-imaged region of the source plane, and we assume a power law source luminosity function  $\phi_L(L) \propto L^{-\beta}$ . Unless otherwise specified, we adopt the source luminosity function of the CLASS survey,  $\beta = 2.1$  (Myers et al. 2003). We take  $\mu$  to be the total magnification of all images, which is appropriate for surveys in which lenses are identified from high-resolution follow-up observations of unresolved targets (including both CLASS and SDSS). We choose coordinates such that the source position  $\mathbf{u}$  is in units of  $\theta_E$ , which means that  $BA$  is naturally (and conveniently) in units of  $\theta_E^2$ .

We compute image separations and biased cross sections using the public software *gravlens* by Keeton (2001b). For each set of  $(\kappa_{\text{ext}}, |\gamma_{\text{ext}}|)$  we place  $10^5$  random sources in the smallest circle enclosing the lensing caustics. We solve the lens equation to find the images, and then compute the image separation and total magnification. Finally, we sum over the multiply-imaged sources to compute the biased cross section.

The next step is to integrate over lens galaxy populations to obtain the total lensing probability. This involves integrating over appropriate distributions of galaxy masses (or velocity dispersions), redshifts, and environments:

$$P = \int dz_l \frac{cdt}{dz_l} (1+z_l)^3 \int d\kappa_{\text{ext}} d|\gamma_{\text{ext}}| p(\kappa_{\text{ext}}, |\gamma_{\text{ext}}|) \times \int d\sigma \frac{dn}{d\sigma} (D_{ol}\theta_E)^2 BA. \quad (4)$$

Here  $D_{ol}$  is the angular diameter distance from the observer to the lens, and  $p(\kappa_{\text{ext}}, |\gamma_{\text{ext}}|)$  is the joint PDF of external convergence and shear from §2. We specify the distribution of galaxy velocity dispersions using the velocity function  $dn/d\sigma$  of early-type galaxies determined from  $\sim 30,000$  galaxies at  $0.01 < z < 0.3$  in the SDSS (Sheth et al. 2003; Mitchell et al. 2005).

The image separation distribution of lensed quasars can then be obtained by differentiating equation (4):

$$\frac{dP}{d\theta} = \int dz_l \frac{cdt}{dz_l} (1+z_l)^3 \int d\kappa_{\text{ext}} d|\gamma_{\text{ext}}| p(\kappa_{\text{ext}}, |\gamma_{\text{ext}}|) \times \int d\hat{\theta} \frac{1}{\hat{\theta}} \frac{d\sigma}{d\theta_E} \frac{dn}{d\sigma} (D_{ol}\theta_E)^2 \frac{d(BA)}{d\hat{\theta}} \quad (5)$$

$$= \int dz_l \frac{cdt}{dz_l} (1+z_l)^3 \int d\kappa_{\text{ext}} d|\gamma_{\text{ext}}| p(\kappa_{\text{ext}}, |\gamma_{\text{ext}}|) \times \int d\hat{\theta} \frac{\sigma}{2\theta} \frac{dn}{d\sigma} \frac{(D_{ol}\theta)^2}{\hat{\theta}^2} \frac{d(BA)}{d\hat{\theta}}. \quad (6)$$

We fix the source redshift to  $z_s = 2.0$  which is a typical redshift for lensed quasars.

## 4 RESULTS

### 4.1 Dependence on convergence and shear

Before presenting results that account for full distribution of convergence and shear, it is useful to study how fixed values

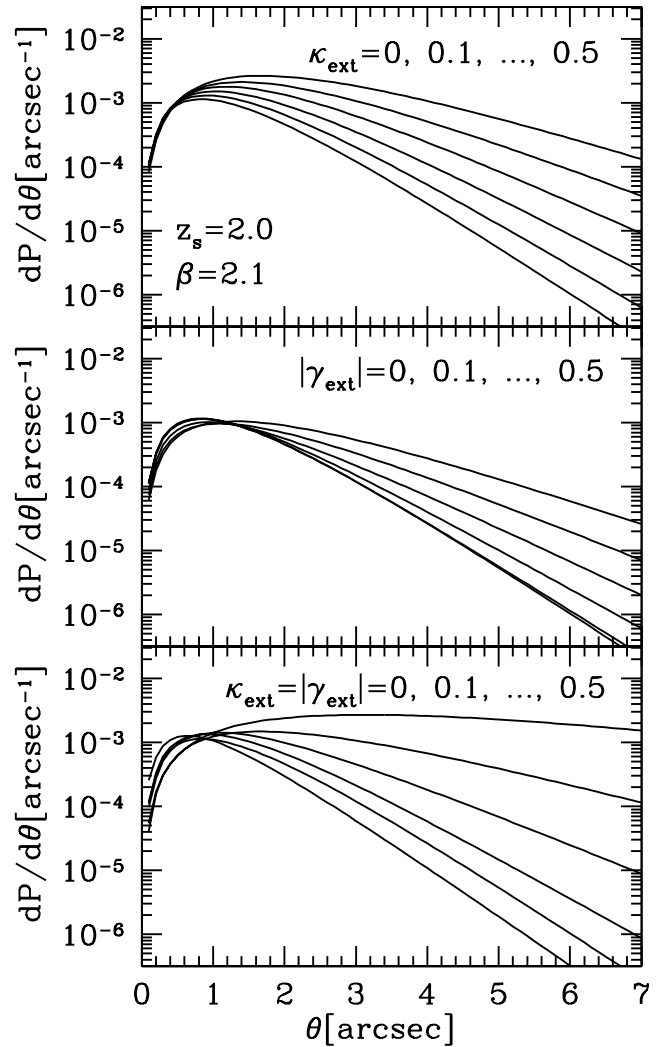


**Figure 4.** Effects of external convergence and shear on the predicted image separation distribution. Here we assume certain fixed values of convergence and/or shear instead of taking account of full joint PDF. Top: We vary the convergence  $\kappa_{\text{ext}}$  from 0 to 0.5 (bottom to top), while the shear is fixed at  $|\gamma_{\text{ext}}| = 0$ . Middle: We vary the shear  $|\gamma_{\text{ext}}|$  from 0 to 0.5 (bottom to top) at  $\theta \gtrsim 1''$ , while the convergence is fixed at  $\kappa_{\text{ext}} = 0$ . Bottom: We set  $\kappa_{\text{ext}} = |\gamma_{\text{ext}}|$  and change the value from 0 to 0.5 (bottom to top at  $\theta \gtrsim 1''$ ).

of  $\kappa_{\text{ext}}$  and/or  $|\gamma_{\text{ext}}|$  affect the image separation distribution. These results are shown in Figure 4.

Convergence and shear both modify the shape of image separation distribution, particularly at relatively large image separations. For instance, at  $\theta = 5''$  a convergence  $\kappa_{\text{ext}} = 0.2$  increases the lensing probability by one order of magnitude, and a shear of  $|\gamma_{\text{ext}}| = 0.2$  enhances it by a factor 2–3. For the same values, convergence clearly has much more effect on lensing probabilities than shear. Combined with the fact that large values of convergence are more likely to occur than large values of shear (see §2), we expect that convergence has the greater impact on image separation distributions.

The results can be understood as follows. First, external convergence magnifies the image plane with respect to the source plane, which increases the image separation by

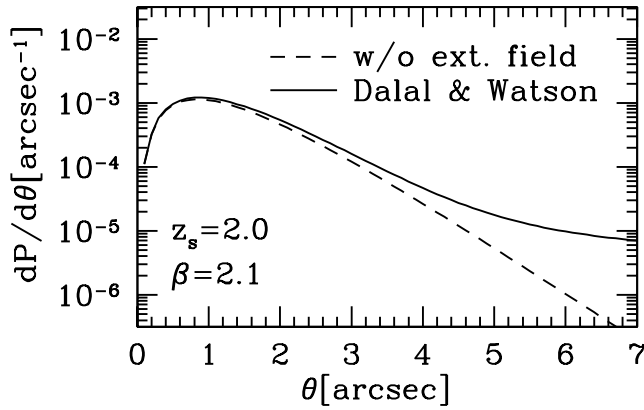


**Figure 5.** Image separation distributions with (*solid*) and without (*dashed*) environmental convergence and shear, calculated from equation (6). We now use the joint distribution of external convergence and shear from Figure 3.

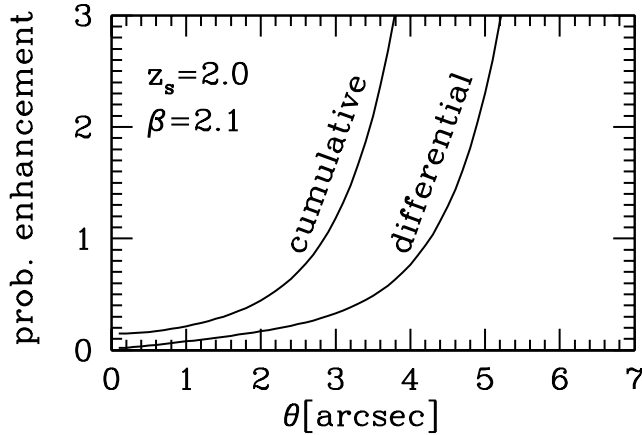


**Figure 6.** Enhancement of the lensing probability as a function of image separation. The enhancement is defined to be  $P_{\text{ext}}/P_0 - 1$ , where  $P_{\text{ext}}$  is the probability with the external field while  $P_0$  is the probability without. We show the enhancement for both the differential lensing probability  $dP/d\theta$  and the cumulative probability  $P(> \theta)$ .

a factor  $(1 - \kappa_{\text{ext}})^{-1}$ . Second, while external convergence does not affect the caustics, it does change the biased cross section by giving additional magnification to the images. Specifically, the biased cross section increases by a factor  $(1 - \kappa_{\text{ext}})^{-2(\beta-1)}$  (see Keeton & Zabludoff 2004). As a result of these two effects, convergence shifts the image separation distribution up and to the right in Figure 4. The increase is significant where the image separation distribution is a decreasing function ( $\theta \gtrsim 1''$ ), but negligible where it is an increasing function ( $\theta \ll 1''$ ). By contrast, shear mainly broadens the image separation distribution. It modestly enhances the lensing probability at  $\theta \gtrsim 1''$ , and suppresses it at  $\theta \lesssim 1''$ .

#### 4.2 Full result

We are now ready to consider the image separation distribution with the full joint PDF of convergence and shear, which

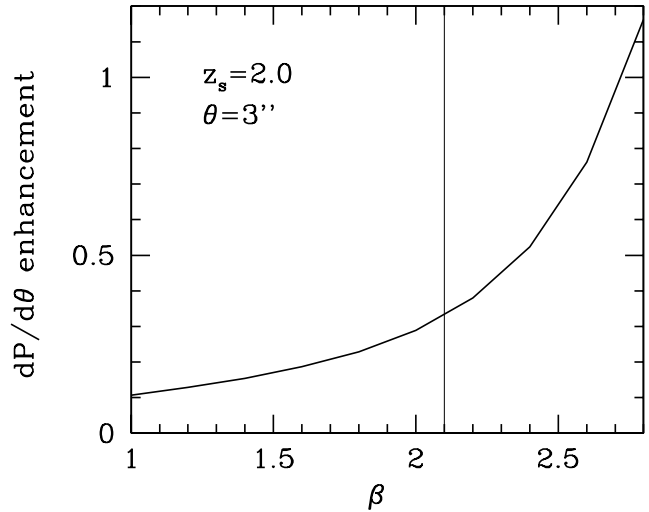


**Figure 7.** Enhancement of the lensing probability, computed at an image separation  $\theta = 3''$ , as a function of the slope  $\beta$  of the source luminosity function. The vertical line indicates the fiducial value we adopt in this paper ( $\beta = 2.1$ , as appropriate for the CLASS lens survey).

is shown in Figure 5. The enhancement of the lensing probability, which is plotted in Figure 6, is small at  $\theta \sim 1''$ , but significant at larger image separations: the increase is  $\sim 30\%$  at  $\theta = 3''$  and  $\sim 200\%$  at  $\theta = 5''$ . Thus, lens galaxy environments are very important when we discuss the shape of the image separation distribution. Indeed, they can account for the excess of lensing probabilities reported by Oguri et al. (2005).

In Figure 6, we also plot the enhancement of the cumulative lens probability  $P(> \theta)$ . We find that the enhancement of the total lensing probability integrated over the all image separation is  $\sim 15\%$ . This enhancement is equivalent to that obtained by shifting the cosmological constant by  $\Delta\Omega_\Lambda \sim 0.05$ , therefore it cannot be ignored in accurate determination of cosmological parameters with lens statistics.

As discussed above, some of the effects of convergence and shear are mediated by magnification bias: convergence directly magnifies images, while shear generates and lengthens the tangential caustic and thus increases the cross section for high magnifications. The enhancement of the lensing probability is therefore expected to depend on the source luminosity function. Indeed, Figure 7 shows that the enhancement at  $\theta = 3''$  increases strongly with the luminosity function slope  $\beta$  (recall  $\Phi \propto L^{-\beta}$ ). This result implies that bright optical lensed quasars with large image separations are more likely to lie in dense environments.

#### 4.3 What enhances the lensing probability?

Dissecting the results further helps us understand the changes to the image separation in more detail. As discussed in §4.1, we believe that convergence is more important than shear because of its stronger effect on the lensing probability (see Fig. 4) and the longer tail to high  $\kappa_{\text{ext}}$  in the joint PDF (see Fig. 3). To check this hypothesis, we project the joint PDF to a distribution of convergence or shear alone (the same distributions shown in Fig. 3 Dalal & Watson 2005)

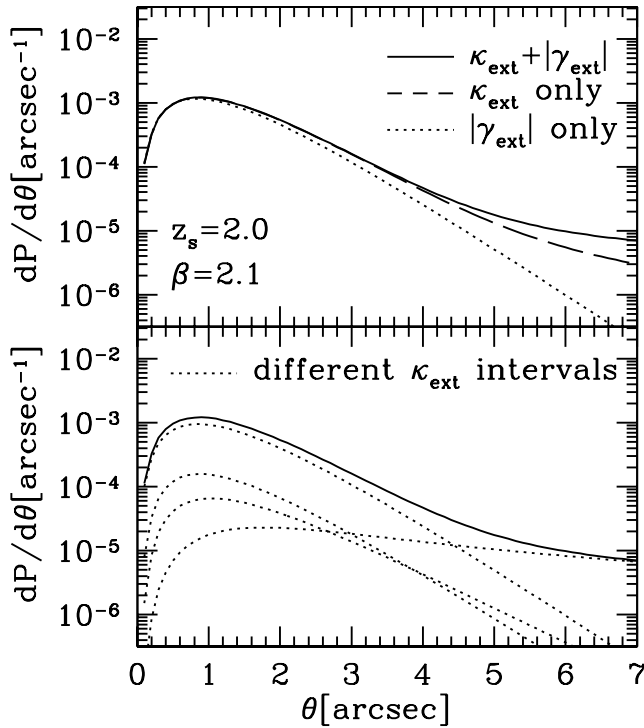


**Figure 8.** Top: Image separation distributions that include only convergence (dashed), only shear (dotted), or both (solid). Bottom: Contributions to the image separation distribution from different  $\kappa_{\text{ext}}$  intervals. From top to bottom (at  $\theta \sim 1''$ ), the dotted curves correspond to  $\kappa_{\text{ext}} < 0.05$ ,  $0.05 < \kappa_{\text{ext}} < 0.15$ ,  $0.15 < \kappa_{\text{ext}} < 0.35$ , and  $0.35 < \kappa_{\text{ext}}$ . The full image separation distribution is shown with the solid line for reference.

and recompute the image separation distribution. The results, shown in the upper panel of Figure 8, confirm that the enhancement of the lensing probability is in fact driven by convergence.

In that case, it is useful to understand what values of  $\kappa_{\text{ext}}$  contribute most to the lensing probability. We see this by decomposing the image separation distribution into contributions from different  $\kappa_{\text{ext}}$  intervals, as shown in the bottom panel of Figure 8. The interpretation depends on the image separation. At small image separations ( $\theta < 3''$ ), most lenses are expected to have small convergences ( $\kappa_{\text{ext}} \lesssim 0.05$ ), and larger and larger convergences are more and more rare. At intermediate separations ( $3'' \lesssim \theta \lesssim 4''$ ), the largest convergences ( $\kappa_{\text{ext}} \gtrsim 0.35$ ) become more important than intermediate values. Finally at large separations ( $\theta \gtrsim 5''$ ), the largest convergences become dominant. In other words, while dense environments with large convergences may be rare, nearly all of the largest separation lenses will be found there.

#### 4.4 Environments of lens galaxies

Figure 8 suggests that the typical environments of lenses are very sensitive to image separation. Put another way, the distribution of convergence and shear for actual lens galaxies will differ from the distribution shown in Figure 3 (which applies to normal elliptical galaxies), by a factor of the lensing probability. To quantify this effect, we derive the

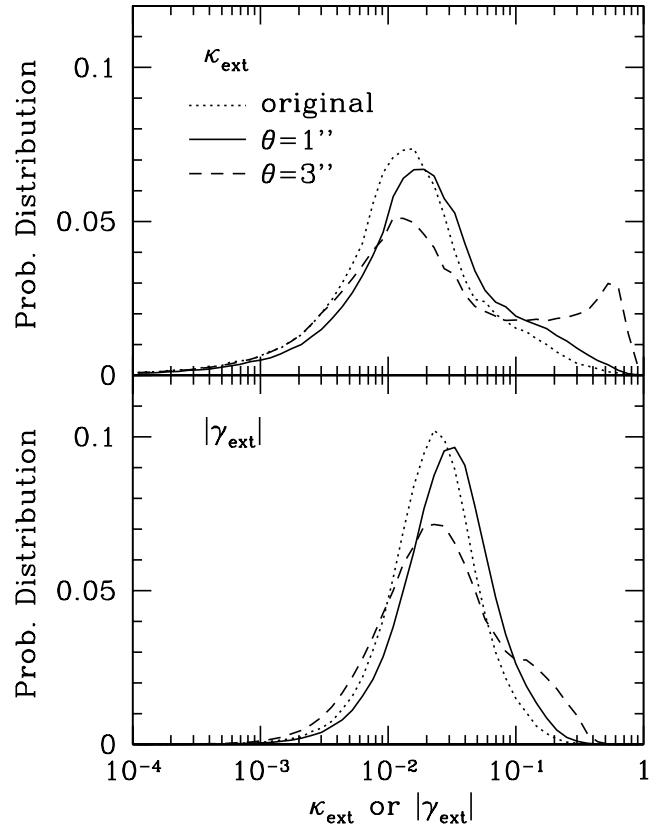


**Figure 9.** Posterior distributions of convergence (top) and shear (bottom), taking into account lensing probabilities. Distributions for lenses with image separations  $\theta = 1''$  (solid) and  $3''$  (dashed) are shown. The original (unweighted) distributions at  $z_l = 0.45$  are shown by dotted lines for reference.

posterior PDF of convergence and shear for lenses at fixed image separations of  $\theta = 1''$  or  $3''$ . Figure 9 shows that the distributions differ from each other, and from the original (unweighted) distributions. The distributions for lenses with  $\theta = 1''$  are similar to the original distributions, just shifted to slightly larger values. However, the distributions for lenses with  $\theta = 3''$  show particularly large increases in the tail of high convergence or shear values.

To see this more clearly, in Figure 10 we show the fraction of lenses with a “strong” environment (defined to be  $\kappa_{\text{ext}}$  or  $|\gamma_{\text{ext}}| > 0.1$ ), as a function of image separation  $\theta$ . The fraction increases monotonically as the image separation grows. For instance, at  $\theta = 1''$  the fraction of lenses with a strong convergence is 11%, while the fraction with a strong shear is 6%. By  $\theta = 3''$  the fractions have increased to 24% and 13%, respectively. (For comparison, the fractions of non-lens elliptical galaxies with strong convergence or shear are just 6% and 3%; see Dalal & Watson 2005.) In other words, the distribution of lens galaxy environments is a strong function of image separation, and this effect should be taken into account when comparing observed environments with theoretical predictions. The increasing fraction of “strong” environments with image separation is qualitatively consistent with the data shown in Figure 1.

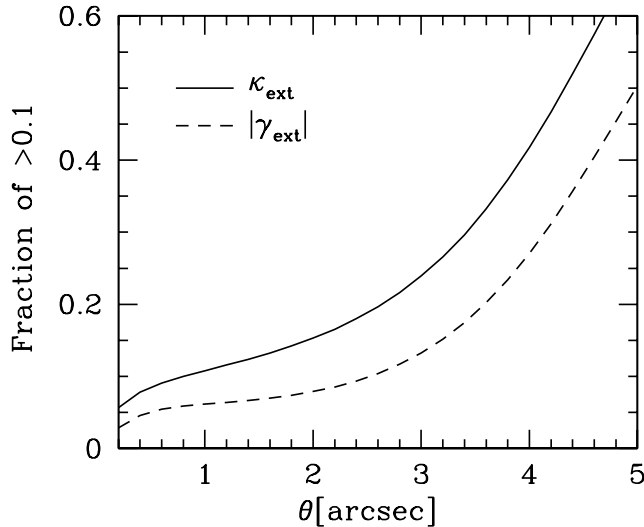


**Figure 10.** Fraction of lenses with “strong” environments (defined by  $\kappa_{\text{ext}}$  or  $|\gamma_{\text{ext}}| > 0.1$ ), as a function of the image separation  $\theta$ .

## 5 SUMMARY AND DISCUSSION

We have studied how the convergence and shear from lens galaxy environments affect lens statistics, in particular the distribution of lens image separations. We find that the external field enhances the lensing probability, especially at large image separations, and the effect increases with the slope of the source luminosity function. We argue that the enhancement is driven mainly by the external convergence, which has been neglected in previous studies of this sort. Our results mesh with those of Keeton & Zabludoff (2004) to indicate that it is essential to include convergence from the environment in order to obtain correct results from both lens modeling and lens statistics. For example, since the external field changes the shape of the image separation distribution rather than its overall amplitude, it will bias attempts to constrain the velocity dispersion function of early-type galaxies using the lens image separation distribution (e.g., Chae 2005).

The environmental boost in the lensing probability depends on the image separation, which means that the posterior distribution of lens environments does as well. The fraction of lenses with a “strong” environment (a convergence or shear larger than 0.1, say) increases monotonically with image separation. Large separation lenses are more likely to be found in dense environments. This bias will be important when comparing the observed distribution of lens environments to theoretical predictions (e.g., Momcheva et al. 2005).

One puzzle remains: even when we take the separation/environment correlation into account, we find that the predicted fraction of lens galaxies with a large shear  $|\gamma_{\text{ext}}| > 0.1$  is  $\sim 10\%$ . However, models of most observed 4-image lenses require shears of  $\sim 0.1$  or larger (Keeton et al. 1997). While 4-image lenses are certainly biased toward dense environments (see Holder & Schechter 2003 for a theoretical perspective, and Momcheva et al. 2005 for intriguing observational results), it does not appear that the bias is strong enough to reconcile our predicted shear distribution with

the “observed” values. At present, it is not clear whether the problem lies with the lens models or the predicted environment distributions. If the latter, then our conclusions regarding the importance of lens galaxy environments should clearly be revisited.

It is also possible that relaxing some simplifying assumptions in our analysis will affect the quantitative results. The most important simplification is the assumption that all galaxies have the same distribution of convergence and shear. As shown in Sheldon et al. (2004), however, the tangential shear signal on scales  $\lesssim 1 h^{-1}$  Mpc increases with increasing velocity dispersion, suggesting that more massive ellipticals reside in denser environments than less massive ellipticals. We expect this effect to enhance the importance of environment for wide-splitting lenses relative to the estimates presented here.

Another simplification was our neglect of lens galaxy ellipticity. The effects of ellipticity are somewhat similar to those of shear (see Huterer et al. 2005), which has a modest effect on the lensing probability. Therefore we expect that our results would not change significantly with the addition of ellipticity. Nevertheless, since ellipticity is important in predictions of the relative numbers of 4-image and 2-image lenses, it will need to be considered more carefully when comparing observed and predicted environment distributions for 4-image lenses alone.

It seems to be too early to say whether there is conflict between the observed and predicted distribution of lens galaxy environments. But it is an intriguing question that deserves to be studied both observationally and theoretically.

## ACKNOWLEDGMENTS

We thank the referee, David Rusin, for helpful comments and suggestions. M. O. is supported by JSPS through JSPS Research Fellowship for Young Scientists. N. D. acknowledges the support of NASA through Hubble Fellowship grant #HST-HF-01148.01-A awarded by the Space Telescope Science Institute, which is operated by the Association of Universities for Research in Astronomy, Inc., for NASA, under contract NAS 5-26555.

## REFERENCES

- Bar-Kana R., 1996, *ApJ*, 468, 17
- Blandford R. D., Surpi G., Kundić T., 2001, in *Gravitational Lensing: Recent Progress and Future Goals*, eds. T. G. Brainerd, & C. S. Kochanek, 65
- Browne I. W. A., et al., 2003, *MNRAS*, 341, 13
- Chae K., 2003, *MNRAS*, 346, 746
- Chae K., Mao S., 2003, *ApJ*, 599, L61
- Chae K.-H., 2005, *ApJ*, 630, 764
- Cohn J. D., Kochanek C. S., McLeod B. A., Keeton C. R., 2001, *ApJ*, 554, 1216
- Dalal N., Kochanek C. S., 2002, *ApJ*, 572, 25
- Dalal N., Watson C. R., 2005, *ApJ*, submitted (astro-ph/0409483)
- Fassnacht C. D., et al., 1999, *AJ*, 117, 658
- Fassnacht C. D., Lubin L. M., 2002, *AJ*, 123, 627

- Fassnacht C. D., et al., 2004, Proceedings of IAU Symposium 225: Impact of Gravitational Lensing on Cosmology (astro-ph/0409086)
- Faure C., Courbin F., Kneib J. P., Alloin D., Bolzonella M., Burud I., 2002, *A&A*, 386, 69
- Faure C., Alloin D., Kneib J. P., Courbin F., 2004, *A&A*, 428, 741
- Fischer P., Schade D., Barrientos L. F., 1998, *ApJL*, 503, L127
- Fukugita M., Futamase T., Kasai M., 1990, *MNRAS*, 246, 24P
- Gorenstein M. V., Shapiro I. I., Falco E. E., 1988, *ApJ*, 327, 693
- Hagen H.-J., Reimers D. 2000, *A&A*, 357, L29
- Hogg D. W., et al., 2003, *ApJ*, 585, L5
- Holder G. P., Schechter P. L., 2003, *ApJ*, 589, 688
- Huterer D., Keeton C., Ma C.-P., 2005, *ApJ*, 624, 34
- Im M., et al., 2002, *ApJ*, 571, 136
- Inada N., et al., 2003, *Nature*, 426, 810
- Johnston D. E., et al., 2003, *AJ*, 126, 2281
- Navarro J. F., Frenk C. S., White S. D. M., 1997, *ApJ*, 490, 493
- Keeton C. R., 2001a, *ApJ*, 561, 46
- Keeton C. R., 2001b, preprint (astro-ph/0102341)
- Keeton C. R., Christlein D., Zabludoff A. I., 2000, *ApJ*, 545, 129
- Keeton C. R., Kochanek C. S., Seljak U., 1997, *ApJ*, 482, 604
- Keeton C. R., Zabludoff A. I., 2004, *ApJ*, 612, 660
- Kneib J., Cohen J. G., Hjorth J., 2000, *ApJL*, 544, L35
- Kochanek C. S., 1996a, *ApJ*, 466, 638
- Kochanek C. S., 1996b, *ApJ*, 473, 595
- Kochanek C. S., et al., 2000, *ApJ*, 543, 131
- Kochanek C. S., White M., 2001, *ApJ*, 559, 531
- Kochanek C. S., Dalal N., 2004, *ApJ*, 610, 69
- Koopmans L. V. E., Treu T., Fassnacht C. D., Blandford R. D., Surpi G., 2003, *ApJ*, 599, 70
- Kundić T., Cohen J. G., Blandford R. D., Lubin L. M., 1997a, *AJ*, 114, 507
- Kundić T., Hogg D. W., Blandford R. D., Cohen J. G., Lubin L. M., Larkin J. E., 1997b, *AJ*, 114, 2276
- McKean J. P., et al., 2005, *MNRAS*, 356, 1009
- Metcalf R. B., Madau P., 2001, *ApJ*, 563, 9
- Mitchell J. L., Keeton C. R., Frieman J. A., Sheth R. K., 2005, *ApJ*, 622, 81
- Möller O., Natarajan P., Kneib J.-P., Blain A. W., 2002, *ApJ*, 573, 562
- Momcheva I., Williams K., Keeton C. R., Zabludoff A., 2005, *ApJ*, submitted
- Morgan N. D., Kochanek C. S., Pevunova O., Schechter P. L., 2005, *AJ*, 129, 2531
- Myers S. T., et al., 2003, *MNRAS*, 341, 1
- Ofek R., Rix H.-W., Maoz D., 2003, *MNRAS*, 343, 639
- Oguri M., 2002, *ApJ*, 580, 2
- Oguri M., et al., 2004, *ApJ*, 605, 78
- Oguri M., et al., 2005, *ApJ*, 622, 106
- Premadi, P., Martel, H., 2004, *ApJ*, 611, 1
- Rusin D., Tegmark M., 2001, *ApJ*, 553, 709
- Rusin D., et al., 2003a, *ApJ*, 587, 143
- Rusin D., Kochanek C. S., Keeton C. R., 2003b, *ApJ*, 595, 29
- Rusin D., Kochanek C. S., 2005, *ApJ*, 623, 666
- Saha P., 2000, *AJ*, 120, 1654
- Schade D., et al., 1999, *ApJ*, 525, 31
- Seljak U., 1994, *ApJ*, 436, 509
- Sheldon E. S., et al., 2004, *AJ*, 127, 2544
- Sheth R. K., et al., 2003, *ApJ*, 594, 225
- Soucail G., Kneib J.-P., Jaunsen A. O., Hjorth J., Hattori M., Yamada, T., 2001, *A&A*, 367, 741
- Tonry J. L., 1998, *AJ*, 115, 1
- Tonry J. L., Kochanek C. S., 1999, *AJ*, 117, 2034
- Tonry J. L., Kochanek C. S., 2000, *AJ*, 119, 1078
- Treu T., Koopmans L. V. E., 2002, *ApJ*, 575, 87
- Turner E. L., Ostriker J. P., Gott J. R., 1984, *ApJ*, 284, 1
- Turner E. L., 1990, *ApJ*, 365, L43
- Young P., Gunn J. E., Oke J. B., Westphal J. A., Kristian J., 1981, *ApJ*, 244, 736
- Zheng Z., et al., 2005, *ApJ*, submitted (astro-ph/0408564)